The *C. elegans* SUN protein UNC-84 interacts with lamin to transfer forces from the cytoplasm to the nucleoskeleton during nuclear migration

Courtney R. Bone*, Erin C. Tapley*, Mátyás Gorjánácz †‡, and Daniel A. Starr*

*Department of Molecular and Cellular Biology, University of California, Davis, CA 95618

†European Molecular Biology Laboratory, 69117, Heidelberg, Germany

‡Present address: Therapeutic Research Group Oncology, Bayer HealthCare Pharmaceuticals, Bayer Pharma AG, 13353, Berlin, Germany

Correspond to: Daniel A. Starr
Department of Molecular and Cellular Biology
1 Shields Ave
University of California
Davis, CA 95618
530-848-5755
dastarr@ucdavis.edu

Running head: SUN-lamin interactions to move nuclei

Abbreviations:		
	LINC	linker of the nucleoskeleton and the cytoskeleton
	SUN	Sad1 and UNC-84
	KASH	Klarsicht, ANC-1, and Syne homology

Abstract

Nuclear migration is a critical component of many cellular and developmental processes. The nuclear envelope forms a barrier between the cytoplasm, where mechanical forces are generated, and the nucleoskeleton. The LINC complex consists of KASH proteins in the outer nuclear membrane and SUN proteins in the inner nuclear membrane that bridge the nuclear envelope. How forces are transferred from the LINC complex to the nucleoskeleton is poorly understood. The *C. elegans* lamin, LMN-1, is required for nuclear migration and interacts with the nucleoplasmic domain of the SUN protein UNC-84. This interaction is weakened by the *unc-84(P91S)* missense mutation. These mutant nuclei have an intermediate nuclear migration defect—live imaging of nuclei or LMN-1::GFP show that many nuclei migrate normally, others initiate migration before subsequently failing, and others fail to begin migration. At least one other component of the nucleoskeleton, the NET5/Samp1/Ima1 homolog SAMP-1, plays a role in nuclear migration. We propose that a nut and bolt model to explain how forces are dissipated across the nuclear envelope during nuclear migration. In this model, SUN/KASH bridges serve as bolts through the nuclear envelope, and nucleoskeleton components LMN-1 and SAMP-1 act as both nuts and washers on the inside of the nucleus.

Introduction

Nuclear migration is essential for a wide variety of cellular processes conserved across eukaryotes including cell migration, cell division, and polarity establishment (Burke and Roux, 2009; Gundersen and Worman, 2013; Morris, 2000; Starr and Fridolfsson, 2010). Nuclear migrations are also central to many developmental processes including fertilization (Reinsch and Gonczy, 1998), neurogenesis (Tsai et al., 2007; Zhang et al., 2009), and muscle development (Bruusgaard et al., 2006). Additionally, nuclear migration is an important process in metastasizing cancer cells (Chow et al., 2012; Fu et al., 2012).

Nuclear migration requires mechanical forces generated by the cytoskeleton to be transferred to the nucleoskeleton, the structural network of the nucleus consisting of lamins, actin, and inner nuclear membrane components (Simon and Wilson, 2011). The nuclear envelope is a specialized extension of the endoplasmic reticulum consisting of an outer nuclear membrane, inner nuclear membrane, and the lumen between the membranes called the perinuclear space (Franke et al., 1981). The inner nuclear membrane is tightly associated with the underlying nucleoskeleton. The unique architecture of the nuclear envelope presents a special challenge to force transfer from the cytoskeleton to the nucleoskeleton.

A nuclear membrane complex of SUN (Sad1 and UNC-84) and KASH (Klarsicht, ANC-1, and Syne homology) proteins, termed the LINC (linker of nucleoskeleton and cytoskeleton) complex, traverses the barrier created by the nuclear envelope and allows for forces generated in the cytoplasm to be transduced into the nucleus (Starr and Fridolfsson, 2010; Tapley and Starr, 2013). SUN proteins are single-pass transmembrane proteins specifically localized to the inner nuclear membrane. They consist of an N-terminal nucleoplasmic domain and a C-terminal domain in the perinuclear space containing the conserved SUN domain (Tapley et al., 2011; Tapley and Starr, 2013; Turgay et al., 2010). The SUN domain functions to recruit KASH proteins to the outer nuclear membrane through a direct interaction between conserved SUN and KASH domains in the perinuclear space (Crisp et al., 2006; McGee et al., 2006; Sosa et al., 2012; Tapley and Starr, 2013). KASH proteins are the only known integral membrane proteins that are specifically localized to the cytoplasmic surface of the nucleus. They are classified by a small conserved KASH peptide at the C-terminus of the protein (Starr and Fridolfsson, 2010; Starr and Han, 2002). The large, cytoplasmic domains of KASH proteins interact with a variety of cytoskeletal elements including microtubule motors, actin, and intermediate filaments (Luxton and Starr, 2014).Thus, KASH proteins interact with the cytoskeleton and then partner with SUN proteins to form a bridge across both membranes of the nuclear envelope, allowing the transfer of force to position nuclei.

Interactions between the cytoskeleton and KASH proteins and between SUN and KASH proteins are relatively well understood (Luxton and Starr, 2014; Tapley and Starr, 2013). However, it is much less clear how SUN proteins interact with the nucleoskeleton. The major component of the nucleoskeleton is the intermediate filament lamin, which provides structure and strength to the nuclear envelope. Vertebrates have two types of lamin proteins; B-type lamins are broadly expressed and A/C-type lamins are expressed in differentiated tissues (Dittmer and Misteli, 2011; Gruenbaum et al., 2005; Simon and Wilson, 2011). A large class of diseases, called laminopathies, has been linked to mutations primarily in lamin A/C (Worman, 2012). Since lamin A/C is involved in disease, most studies on interactions between lamins and SUN proteins have focused on lamin A/C rather than the more broadly expressed lamin B. Therefore, how SUN proteins interact with the nuclear lamina and especially lamin B remains an

open question. Here we test the hypothesis that SUN proteins interact with lamin B during nuclear migration.

Reports of interactions between SUN proteins and lamin A/C are limited to *in vitro* GST pull-down assays and FRAP and FRET assays in transfected tissue culture cells. These data show that SUNs interact with lamin A/C, but conflict as to whether mammalian SUN1 or SUN2 bind more tightly (Crisp et al., 2006; Ostlund et al., 2009). Other studies show that some lamin A disease mutations disrupt the ability of lamin A to bind SUN proteins, while other mutations increase the interaction between lamin A and SUN1 (Haque et al., 2010). Nonetheless, SUN proteins properly localize to the nuclear envelope in lamin A mutant cells (Chen et al., 2012; Crisp et al., 2006; Haque et al., 2010). Lamin A is also required for nuclear migrations in polarizing fibroblasts (Folker et al., 2011). Depletion of SUN1 in lamin A knockout mice increases longevity and the health of the mice, suggesting that the interaction between lamin A and SUN1 is important in the progression of laminopathies (Chen et al., 2012; Chen et al., 2014). One possible explanation for this finding is that by removing SUN1, the forces transferred to the weakened nucleoskeleton are reduced, which may lead to less mechanical damage to already fragile nuclei (Starr, 2012). Such a model fits well with our hypothesis that SUN proteins interact with lamins to move nuclei.

SUN protein interactions with lamin B are less well understood at a biochemical level than their lamin A/C counterparts. In *C. elegans* and *Drosophila*, lamin B is required for the localization of SUN proteins (Kracklauer et al., 2007; Lee et al., 2002). However, it is not clear the extent to which SUN localization to the nuclear envelope requires a direct interaction with lamin B. There is conflicting evidence in the literature as to whether or not lamin B interacts with mammalian SUN1 or SUN2 by *in vitro* pull-down assays (Crisp et al., 2006; Haque et al., 2006). However, two important developmental genetic experiments suggest that lamin B functions in some of the same nuclear migration events as SUN and KASH proteins. Mice with knockout mutations in lamin B2 have nuclear migration defects in the central nervous system similar to SUN and KASH knockout defects (Coffinier et al., 2010a; Coffinier et al., 2010b; Coffinier et al., 2011; Zhang et al., 2009). Similarly, null mutations in the *Drosophila* lamin B gene *Lam* Dm_o cause a nuclear migration defect in the developing eye disc very similar to SUN and KASH mutants (Kracklauer et al., 2007; Patterson et al., 2004). Taken together, these data are consistent with a model where SUN proteins interact with lamin B to mediate nuclear migration.

Here we utilized nuclear migration in *C. elegans* embryonic hypodermal cells (Starr and Han, 2005; Zhou and Hanna-Rose, 2010) as a model for studying the interaction between SUN proteins and lamins. *C. elegans* has a single lamin gene, as compared to three to four lamins in vertebrate systems. Invertebrate lamins are widely considered as B-type lamins, but unrooted phylogenetic trees place invertebrate lamins in their own clade nearly equal distance from vertebrate lamin As and Bs (Dittmer and Misteli, 2011; Liu et al., 2000). Having a single lamin gene is both an advantage and a disadvantage for this study. It makes the study feasible, but complicates the significance of the study when thinking about vertebrate cells. The *C. elegans* lamin protein LMN-1, also known as Ce-lamin and CeLam-1, is broadly expressed and required for early embryonic cell divisions; *lmn-1(RNAi)* embryos die at around the 100 cell stage with multiple mitotic defects (Liu et al., 2000). Furthermore, only one SUN protein, UNC-84, is present in the cell at the time of hyp7 nuclear migration (Fridkin et al., 2004; Minn et al., 2009; Wang et al., 2009). Finally, *C. elegans* hyp7 nuclear migration is amenable to the use of many genetic and live-imaging tools (Fridolfsson et al., 2010; Fridolfsson and Starr, 2010; Starr et al.,

2001). Here we combine *C. elegans* genetics and yeast two-hybrid assays to test our hypothesis that the SUN protein UNC-84 binds to the lamin B protein LMN-1. Furthermore, we employ live imaging to carefully describe the nuclear migration phenotypes of *unc-84* mutants that disrupt the interaction with lamin B. Our data strongly support that SUN proteins bind directly to lamin B to transfer forces generated in the cytoskeleton to the nucleoskeleton, thus facilitating nuclear migration.

Results

Mutations in the nucleoplasmic domain of UNC-84 lead to an intermediate nuclear migration defect.

Null mutations in *unc-84* cause a complete block of nuclear migration in hyp7 precursors resulting in about 14 nuclei residing abnormally in the dorsal cord of larvae (Figure 1) (Fridolfsson and Starr, 2010; Malone et al., 1999). However, three alleles, *unc-84(e1411*, *e1174*, and *n322)*, were originally reported to cause an intermediate hyp7 precursor nuclear migration defect (Malone et al., 1999). Normally, nuclei migrate across the length of the dorsal hyp7 precursors during *C. elegans* embryogenesis. After the bulk of embryonic cell division and just prior to the initiation of morphogenesis, 15 dorsal epithelial cells intercalate and their nuclei migrate across the dorsal midline to the contralateral side of the embryo (Figure 1A) (Sulston et al., 1983). Nuclei are pulled along polarized microtubules by kinesin-1 and dynein, which are recruited to the surface of the nuclear envelope by the KASH protein UNC-83 (Fridolfsson et al., 2010; Fridolfsson and Starr, 2010; Meyerzon et al., 2009a). These cells subsequently fuse to form the embryonic dorsal hyp7 syncytium (Altun, 2009; Sulston et al., 1983). Mutations that block nuclear migration in hyp7 precursors result in nuclei abnormally residing in the dorsal cord of newly hatched L1 larvae, having been pushed there by underlying body wall muscles (Figure 1A) (Malone et al., 1999; Sulston and Horvitz, 1981). About 90% of the nuclei that fail to migrate end up in the dorsal cord (Fridolfsson and Starr, 2010).

The *unc-84* alleles *e1411*, *e1174*, and *n322* resulting in an intermediate hyp7 precursor nuclear migration defect all disrupt the N-terminal nucleoplasmic domain of UNC-84. *unc-84(e1411)* is a P91S missense mutation, *unc-84(e1174)* is a deletion removing residues 40-161 of UNC-84, and *unc-84(n322)* is a small deletion of the ATG and is predicted to use the ATG at residue 209 (Figure 1H) (Malone et al., 1999).We will henceforth refer to these alleles as *unc-84(P91S)*, *unc-84(Δ40-161)*, and *unc-84(Δ1-208)*.

In order to quantify partial nuclear migration defects, a transgenic line expressing nuclear GFP specifically in hypodermal nuclei (*ycIs10[*$p_{col\text{-}10}$*nls::gfp::lacz]*) was created. The *unc-84* alleles *P91S*, *Δ40-161*, and *Δ1-208* caused nuclear migration defects where 7.3±0.4, 10.3±0.5, and 8.6±0.5 (mean±95%CI; Figure 1B,E-G) nuclei fail to migrate, respectively. This intermediate phenotype is significantly different from either the null allele *unc-84(n369)* where 13.9±0.4 nuclei failed to migrate or wild-type animals where only 0.1±0.1 nuclei were mispositioned to the dorsal cord (Figure 1). The intermediate nuclear migration defect of at least *unc-84(P91S)* is unlikely due to a reduction in the levels of the mutant UNC-84 protein as compared to wild type. Quantification of immunofluorescence intensity showed that approximately equal levels of UNC-83 protein were found at the nuclear envelope in both the *unc-84(P91S)* mutant and wild-type embryos (Supplementary Figure 1). Because *unc-84(n369)* null mutations disrupt both migration and anchorage (Malone et al., 1999), we next asked the

extent to which these three mutant lines caused any anchorage defects. The nuclei that failed to migrate and are abnormally found in the dorsal cord of the hyp7 syncytium are usually clumped together in *unc-84(n369)* mutant larvae (Figure 1D). We classified a nuclear anchorage defect (Anc^-) if an L1 larva had a row of at least 3 nuclei touching each other. In the null *unc-84(n369)* allele, 43% (n=14) of larvae were Anc^-. In contrast 0% of *unc-84(P91S)*, 6% of *unc-84(Δ40-161)*, and 0% of *unc-84(Δ1-208)* L1 larvae were Anc^- ($n \geq 30$). Our data therefore suggest that disruption of the nucleoplasmic domain of UNC-84 results in partial nuclear migration, but not nuclear anchorage, defects.

The nucleoplasmic domain of UNC-84 binds to lamin.

We hypothesized that the P91S mutation in the nucleoplasmic domain of UNC-84 disrupted an interaction between UNC-84 and some unknown component of the nucleoskeleton. A yeast two-hybrid screen of a *C. elegans* mixed stage cDNA library was conducted to identify proteins interacting with the nucleoplasmic domain of UNC-84. The first 385 amino acids of UNC-84 fused to the GAL4 DNA binding domain was used as bait. This construct incorporates the majority of the nucleoplasmic domain of UNC-84 upstream of the transmembrane domain located at residues 512-532 (Figure 1H) (Tapley et al., 2011). Approximately $4x10^6$ yeast clones were screened and the prey inserts of 106 positive colonies were sequenced. 16 different proteins were identified as potential interacting partners of UNC-84. LMN-1, the sole *C. elegans* lamin protein (Liu et al., 2000), was found in 16 independent clones. No other known component of the nucleoskeleton was identified.

We used the yeast two-hybrid assay to further map the LMN-1 interaction domain of UNC-84 (Figure 2A). The assay was repeated five times with UNC-84 1-385 and the empty vector to verify the interaction. The other constructs containing smaller regions of UNC-84 were examined at least twice. The original bait used for the screen, UNC-84(1-385), strongly interacted with the LMN-1 prey. A smaller bait, UNC-84(1-100) also interacted with LMN-1. However, UNC-84(1-59), UNC-84(59-385) and UNC-84(385-510) did not interact with LMN-1. These data suggest the minimal interaction domain is somewhere in the first 100 amino acids of UNC-84. Interestingly, all three *unc-84* alleles with the intermediate hyp7 nuclear migration phenotype disrupt this portion of UNC-84 (Figure 1H). We therefore tested the hypothesis that the *unc-84(P91S)* mutation disrupted the two-hybrid interaction with LMN-1. Quantitative β-galactosidase liquid assays were used to measure the yeast two-hybrid interaction between LMN-1 and wild type or P91S mutant UNC-84. The P91S mutation significantly reduced the strength of the interaction between LMN-1 and UNC-84, as determined by student t-tests (Figure 2B).

***lmn-1(RNAi)* leads to a nuclear migration defect**

The yeast two-hybrid data are consistent with a hypothesis that the *unc-84(P91S)* intermediate nuclear migration defect is due to a reduced interaction between UNC-84 and LMN-1. One prediction of this model is that disruptions of *lmn-1* should lead to similar nuclear migration defects. *lmn-1* is an essential gene required for the earliest embryonic cell divisions. Adults fed dsRNA against *lmn-1* for over 24 hours produce embryos that have small pronuclei and chromosomal segregation defects, leading to embryonic lethality before the 100-cell stage (Liu et al., 2000; Meyerzon et al., 2009b). To study the effect of *lmn-1(RNAi)* later in embryogenesis, at the time of nuclear migration in hyp7 precursors, we fed young adults dsRNA against *lmn-1* over shorter windows, which allowed for the survival of 10 to 40 larvae per mother. These larvae demonstrated a nuclear migration defect where screening a total of 121

larvae from four different experiments resulted in an average of 2.4±0.5 (mean±95%CI) hyp7 nuclei in the dorsal cord (Figure 3). An example of an animal with an approximately 50% hyp7 nuclear migration failure is depicted in Figure 3B. The *lmn-1(RNAi)* hyp7 nuclear migration failure is statistically more severe than wild type (p <0.0001 when using an unpaired t-test with Welch's correction). The number of nuclei in the dorsal cord per animal ranges from zero to ten. The range is large because individuals with no nuclei in the dorsal cord were likely subjected to little or no dsRNA, leading to incomplete knockdown of *lmn-1*. Finally, *lmn-1(RNAi)* treatment of the three UNC-84 N-terminal mutant lines resulted in minor enhancement. Given the hypomorphic nature of both the N-terminal mutations and *lmn-1(RNAi)*, this is consistent with our model that UNC-84 and LMN-1 function in the same pathway. This enhancement was not significant for either of the two deletion alleles, *unc-84(Δ40-161)* increased by an average of 0.35 nuclei and *unc-84(Δ1-208)* increased by an average of 0.45 nuclei. The average enhancement in u*nc-84(P91S*) of 1.9 nuclei was significant (p<0.0001 with student t-test), but did not increase to anywhere near the levels observed in *unc-84(null)* animals.

LMN-1 is part of a network of *C. elegans* proteins at the nucleoskeleton including the Baf homolog BAF-1 and the LEM proteins *emr-1* and *lem-2* that are thought to function in a mutually dependent network. Mutations in *baf-1* or *emr-1; lem-2* double mutations have identical early embryonic phenotypes as *lmn-1(RNAi)* (Liu et al., 2003; Margalit et al., 2005; Meyerzon et al., 2009b). We therefore examined the extent to which *baf-1*, *emr-1*, and *lem-2* functioned similarly to *lmn-1* during nuclear migration in hyp7 precursors. We observed the previously reported early embryonic lethality in *baf-1(RNAi)* and *lem-2(tm1582); emr-1(RNAi)* embryos (data not shown). However, when fed dsRNA for shorter periods of time as in our *lmn-1(RNAi)* experiment, we did not observe any nuclear migration defects in *baf-1(RNAi)* or *lem-2(tm1582); emr-1(RNAi)* larvae (Figure 3A). We therefore conclude that LMN-1 functions independently of BAF-1 and the LEM proteins during embryonic hyp7 nuclear migration.

Live imaging of the partial nuclear migration defect in *unc-84(P91S)* embryos

We envisioned three possible ways that the *unc-84(P91S)* mutation could partially disrupt nuclear migration. First, half the nuclei could migrate normally, while the other half fail to even initiate nuclear migration. Alternatively, *unc-84(P91S)* mutant nuclei could migrate at a slower velocity than wild-type nuclei where only half finish migration in the available period of time. Finally, *unc-84(P91S)* mutant nuclei might initiate nuclear migration at the normal time and velocity, and then fail at some point later in nuclear migration. To distinguish between these possibilities, *unc-84(P91S)* mutant nuclei were observed by time lapse imaging during hyp7 precursor development. Time-lapse imaging of hyp7 nuclear migration in wild type, *unc-84(null)*, or microtubule motor mutant embryos has previously led to great insights on the mechanisms of nuclear migration (Fridolfsson and Starr, 2010; Starr, 2011; Zhang and Han, 2010). For example, see our previous studies for details on wild type and *unc-84(null)* nuclear migrations (Fridolfsson and Starr, 2010). Here we employed both DIC microscopy and fluorescence imaging of LMN-1::GFP to follow nuclear migration in a subset of hyp7 precursor cells on the dorsal surface of the embryo (Figures 1A and 4A-D; hyp7 precursors 11–16, following designations of Sulston et al., 1983). Nuclear migration defects in wild type, *unc-84(null)*, and *unc-84(P91S)* embryos were quantified by four different assays. For the first three assays, DIC time-lapse microscopy was used to characterize the complete nuclear migration in embryonic hyp7 precursors (Figure 4A-D). Images were taken at 15 sec intervals over 35-50 min. Representative time-lapse movies of wild type, *unc-84(null)*, and *unc-84(P91S)* embryos at

the time of nuclear migration are shown in Supplemental Movies 1-3.

Nuclear migration events were scored as normal if full contralateral movement was completed within 30 minutes, partial if migration initiated but failed to complete, or static if initiation did not occur (Figure 4E). See Supplemental Movie 3 for an example of a static nucleus (white arrowhead) and a nucleus that partially migrated (black arrowhead) in an *unc-84(P91S)* embryo. 100% of wild-type nuclei completed their migrations normally. 80% of the *unc-84(null)* nuclei were static while 20% had partial migrations. The *unc-84(P91S)* nuclei had an intermediate phenotype where 63.8% of nuclei migrated normally, 20.7% initiated but failed to complete migration, and 15.5% were static.

The time it took a nucleus to reach the midline was also analyzed (Figure 4F). We previously showed that wild-type nuclei reached the midline at about 11 minutes after intercalation while most *unc-84(null)* nuclei failed to reach the midline and those that did took an average of 37 minutes (Fridolfsson and Starr, 2010). Here, the time a migrating nucleus took to reach the midline was binned into less than 10 min, 10-30 min, over 30 min, or not within the length of the film (films were 35-50 min). Late during filming, embryos began to rotate in the egg shell. This often resulted in the midline moving to or past a subset of nuclei, thus making the *unc-84(null)* phenotype described in Figure 4F appear less severe than the phenotype presented in Figure 4E. Consistent with our previous results, the *unc-84(P91S)* mutant nuclei had an intermediate defect; 27% migrated to the midline in less than 10 min, but 25% took longer than 30 min or never reached the midline. This intermediate phenotype was significantly different from wild type or *unc-84(null)* nuclei as determined by χ^2 contingency tests (Figure 4F).

As a third assay, the distance nuclei moved in the first 10 minutes of migration was binned into half μm increments and plotted (Figure 4G). Wild-type nuclei moved an average of 2.7±0.4 μm and had the highest frequency of nuclei that migrated 2.6-3.0 μm in the first 10 min of migration (blue in Figure 4G). *unc-84(null)* nuclei migrated an average of 1.2±0.3 μm and were shifted greatly toward the three lowest categories that migrated less than 1.5 μm in 10 min (green in Figure 4G). *unc-84(P91S)* nuclei migrated an average of 1.9±0.4 μm, which is statistically less than wild-type movements (p=0.005 in a t-test) and more than *unc-84(null)* nuclei move (p=0.016).

To visualize changes in nuclear envelope morphology over shorter time frames, time-lapse fluorescence imaging was performed to follow LMN-1::GFP in migrating nuclei. A transgenic line expressing *lmn-1::gfp* under the control of a hypodermal-specific promoter from an extra-chromosomal array (Fridolfsson and Starr, 2010) was crossed to *unc-84(P91S)* and *unc-84(null)* animals. Embryos at the stage where hyp7 nuclear migration would normally occur were identified using DIC microscopy. LMN-1::GFP was then imaged in these embryos at one-second intervals for 3 to 9 minutes to follow changes in nuclear envelope morphology during nuclear migration. Movies of LMN-1::GFP in wild type, *unc-84(null),* and *unc-84(P91S)* embryos were visually different (Supplemental Movies 4-6). Nuclei in wild-type embryos underwent large movements, greater than half the width of a nucleus, and were almost constantly moving (Figure 5A, Supplemental Movie 4). In contrast, *unc-84(null)* nuclei tended to remain in place over several minutes of filming (Figure 5B, Supplemental Movie 5); most movements were due to the drift of the entire embryo within its eggshell. Interestingly, in *unc-84(P91S)* nuclei, both phenotypes were visualized. Some nuclei were observed undergoing large directional movements of up to 1 μm/min, while other nuclei did not move at all.

To categorize the movements of LMN-1::GFP during nuclear migration, projections were made combining each frame of an 8 min 20 sec time-lapse series (Figure 5 A'-C'). The projections were split into three colors to show the direction of movement. Magenta signifies the first third of the series, yellow the second, and cyan the last third of the series. Using the time-lapse projections of LMN-1::GFP, nuclei were binned into three categories based on the size of an individual nuclear projection (Figure 5D-F). To better visualize movement, insets show the nuclei identified in the projections in the first frame (magenta) and the last frame (cyan) of the film. Many nuclei had large directional movements over the course of imaging, as visualized by the lack of overlap between the initial and final positions of the nucleus of at least half the width of the nucleus (arrow and inset in Figure 5A'; green in Figure 5D-F). Other nuclei that moved small amounts, but the projections remained mostly circular were classified as small movements. Finally, nuclei that did not move in up to 9 minutes of imaging were scored as static when the time-lapse projection remained circular and when the projection was split into thirds, the colors merged to white (arrow in Figure 5B'). The same identified nucleus is shown in the inset, this demonstrates slight embryo drift, as the first and last images are not directly super-imposed (inset in Figure 5B'). In summary of these data, 72% of wild-type nuclei moved large distances while 28% had small movements (figure 5D). 76% of *unc-84(null)* nuclei did not move, while the remaining 24% had only small movements (Figure 5E). In *unc-84(P91S)* animals, large movements were seen 61% of the time and small movements were seen in 35% of nuclei; the remaining 4% of nuclei did not move (Figure 5F). Our LMN-1::GFP movement assay demonstrated statistically significant differences when comparing *unc-84(null)* nuclear migrations to both wild type and *unc-84(P91S)* embryos ($p < 0.0001$ using a χ^2 contingency test). However, wild type and *unc-84(P91S)* were not significantly different ($p=0.4$). The lack of statistical significance may result from the relatively short duration of the time-lapse series, such that only a snap shot of nuclear migration was visualized as compared to the longer analyses in Figure 4. Nonetheless, the *unc-84(P91S)* phenotype followed the trend of intermediate nuclear migration phenotypes. Multiple time-lapse series were taken of some embryos. Occasionally *unc-84(P91S)* nuclei were observed to move in one series, but then failed to migrate in the subsequent series (arrowhead and insets in Figure 4C'-C"). In another *unc-84(P91S)* time-lapse movie, a nucleus was observed where a large and rapid invagination appeared to push the nucleus just before the time of nuclear migration initiation (Supplemental movie 7). This rapid change may have resulted from abrupt microtubule motor activity acting against a weakened UNC-84 to LMN-1 interaction. Together, these data are consistent with our hypothesis that a weakened connection between UNC-84 and LMN-1 could lead to a nucleus that initiates migration normally, but then fails to complete its migration.

The inner nuclear membrane component SAMP-1 functions during nuclear migration.

In our working model, forces generated in the cytoplasm are transmitted across the nuclear envelope by SUN/KASH bridges and then dissipated across the nucleoskeleton by lamin. The nucleoskeleton consists of lamins, scores of inner nuclear membrane proteins, and other proteins that mediate interactions between the nuclear envelope and chromatin (Simon and Wilson, 2011). We therefore hypothesized other components of the nucleoskeleton play roles in connecting the nucleus to the nuclear envelope to allow for force dissipation during nuclear migration. An attractive candidate to play such a role is the Samp1/NET5/Ima1 *C. elegans* homolog T24F1.2 we named SAMP-1. The mammalian putative ortholog was originally found in a proteomic screen for integral components of the inner nuclear membrane and named NET5 (Schirmer et al., 2003). NET5 was subsequently named Samp1 and shown to play a role in

positioning nuclei in polarizing NIH 3T3 cells. Nuclear migration in polarizing mouse NIH3T3 cells relies on SUN-KASH bridges to couple moving actin arrays in the cytoplasm to the nucleoskeleton (Folker et al., 2011; Luxton et al., 2010). This nuclear migration also requires Samp1, which partially co-localizes and co-immunoprecipitates with SUN proteins in transmembrane actin-associated nuclear, TAN, lines (Borrego-Pinto et al., 2012). The homologous protein in *S. pombe*, Ima1, interacts in yeast two-hybrid assays with the SUN protein Sad1 and has been implicated in the maintenance of nuclear morphology (Hiraoka et al., 2011). Previously, a broad bioinformatics study predicted that *C. elegans* SAMP-1 would be a component of the nuclear envelope and confirmed this localization in the early embryo using a transgenic SAMP-1::GFP fusion protein (Gunsalus et al., 2005). However, nothing else is known about the function of *C. elegans* SAMP-1. We therefore set out to examine the role of *C. elegans* SAMP-1 in nuclear migration.

We first characterized the intracellular localization pattern of endogenous SAMP-1 to see if it was plausible that SAMP-1 functions at the nuclear envelope during nuclear migration in embryonic hyp7 precursor. Antibodies were raised against the C-terminus of SAMP-1. Anti-SAMP-1 antibodies recognized a band of the predicted size on a western blot. The band intensity was greatly reduced in *samp-1(RNAi)* extracts (Supplemental Figure 2). SAMP-1 antibodies localized strongly to a ring around DAPI-stained nuclei, consistent with nuclear envelope staining, in all cells of wild-type early embryos, but not in *samp-1(tm2710)* likely null embryos (Figure 6, Supplemental Figure 2). Therefore, the antibody is specific for SAMP-1 with a localization pattern expected for a nuclear membrane protein. While we did not test the specific localization within the nuclear envelope, we hypothesize SAMP-1 is an inner nuclear membrane protein based on the published localization of the mouse ortholog, Samp1 (Buch et al., 2009). In later embryos at the time of hyp7 nuclear migration, SAMP-1 localization at the nuclear envelope was less strong and limited to a subset of cells that included hyp7 precursors (Figure 6C-D).

In mammalian tissue culture, Samp1 requires LaminA/C for localization to the nuclear envelope (Borrego-Pinto et al., 2012). It has also been demonstrated that *C. elegans* UNC-84 requires LMN-1 for nuclear envelope localization (Lee et al., 2002). Surprisingly, SAMP-1 localized to the nuclear envelope in *lmn-1(RNAi)* embryos (Figure 7). In both early embryos (Figure 7A-B) and embryos around the time of migration (Figure 7C-D) that SAMP-1 was able to localize in lamin knockdown animals, while UNC-84 was not. LMN-1 staining was used as a control to confirm that the *lmn-1(RNAi)* knockdown was efficient.

After showing that SAMP-1 localizes to the nuclear envelope in migrating nuclei, we tested the extent to which SAMP-1 functions to move nuclei. Homozygous *samp-1(tm2710)* were embryonic lethal. We therefore fed *samp-1(tm2710)/+* adults dsRNA against *samp-1* for 48-72 hours and examined their offspring. Nuclei abnormally located in the dorsal cord were counted in 266 *samp-1(tm2710)/+; samp-1(RNAi)* L1 larvae. On average, 0.4±0.1 nuclei (mean+/-95%CI) were observed in the dorsal cord (Figure 6G-I), which is statistically significantly when compared to wild type (p=0.005 by unpaired t test with Welch's correction). Occasionally, *samp-1(RNAi)* L1 larvae had up to 5 nuclei per worm that failed to migrate (Figure 6G). We therefore concluded that *samp-1* plays a small, but significant role in nuclear migration.

Discussion

The results presented here combine genetic analyses, time-lapse imaging of nuclear migration, and a yeast two-hybrid screen. Together, the data provide mechanistic insights into both the molecular interaction between the SUN protein UNC-84 and lamin as well as the functional implications of disruption of this interaction during nuclear migration. We showed alleles disrupting the N-terminal nucleoplasmic domain of UNC-84 led to an intermediate nuclear migration defect. We then performed a yeast two-hybrid screen to find candidate interacting partners of the nucleoplasmic domain of UNC-84. Interestingly, we identified an interaction between UNC-84 and the *C. elegans* lamin protein LMN-1. Furthermore, the point mutation UNC-84(P91S) that led to an intermediate nuclear migration phenotype also disrupted the interaction between UNC-84 and LMN-1. As predicted from these data, *lmn-1(RNAi)* led to a similar nuclear migration defect. Knockdown of another member of the nucleoskeleton, *samp-1*, led to a weak nuclear migration phenotype. Nuclear migrations in *unc-84(P91S)* embryos were carefully analyzed by time-lapse imaging to provide insight into the intermediate nuclear migration defect. Some nuclei in the *unc-84(P91S)* mutant background migrated normally, while others failed. Of the failed nuclei, many initiated migration normally before stopping part way through migration, while others failed to move at all. Interestingly, we did not see slow moving nuclei in *unc-84(P91S)* embryos, the nuclei that did move did so similarly to wild-type nuclei.

Our proposed model is shown in Figure 8. In this model, KASH/SUN bridges serve as molecular bolts through the nuclear envelope to transfer forces generated in the cytoplasm across the nuclear envelope. UNC-83 on the cytoplasmic surface of the nuclear envelope interacts with microtubule motors kinesin-1 and dynein (Fridolfsson et al., 2010; Meyerzon et al., 2009a). The forces generated by the motors are transmitted across the outer nuclear membrane by UNC-83 and then to the SUN protein UNC-84 through an interaction between KASH and SUN domains (Sosa et al., 2012; Tapley and Starr, 2013). Finally, UNC-84 spans the inner nuclear membrane (Tapley et al., 2011) and interacts with lamin (Figure 2) to complete the connection between the cytoskeleton to the nucleoskeleton (Figure 8A). However, the amount of force that can be transferred across the nuclear envelope by the KASH/SUN molecular bolt without stabilization by an interaction with the nucleoskeleton is limited. It is useful to think of this complex as a nut and bolt in drywall (Figure 8B), where the interaction of UNC-84 with nucleoskeletal components dissipates forces across a larger area along the inside of the wall, reducing the likelihood of failures under tension. In our model, LMN-1 functions as a key component of the molecular nut and washer to dissipate the forces transmitted across the KASH/SUN bolt to structural elements inside the nucleus. The LMN-1 nut and washer is only as strong as its interaction with the UNC-84 nucleoplasmic domain of the bolt. If the UNC-84 to LMN-1 interaction fails, as in the UNC-84(P91S) mutant, the nucleus could continue to migrate for some time without lamin serving as a nut and washer. However, at some critical point the forces are too strong, and the KASH/SUN bolt is catastrophically detached, leading to a failure in nuclear migration. The stability of the bolt depends on many factors. It is therefore difficult to predict when the KASH/SUN bridge will fail, explaining why some UNC-84(P91S) nuclei fail at the initiation of migration, while others migrate part way before stalling, and many successfully complete migration. While the LMN-1 nut is required to ensure normal nuclear migration, it does not appear necessary for nuclear anchorage, because *unc-84(P91S)* nuclei are normally anchored (Figure 1) (Malone et al., 1999).

It is difficult to translate our findings from the *C. elegans* system, where there is a single lamin, to vertebrate cells where there are three to four lamins. However, mutations in lamins in other developmental systems lead to nuclear migration phenotypes consistent with our model. Mice carrying knockout mutations in laminB2 have nuclear migration defects in the developing central nervous system similar to defects in SUN or KASH mutant mice (Coffinier et al., 2010b). Likewise, mutations in *Drosophila Lam* Dm_o have nuclear migration defects in the developing eye disk similar to SUN and KASH mutants (Patterson et al., 2004). Furthermore, heterozygous, dominant loss-of-function mutations in *Drosophila Lam* Dm_o were identified as enhancers of phenotypes caused by overexpression of the KASH protein in the developing eye disc, suggesting that the function of SUN-KASH bridges are sensitive to the levels of lamin (Patterson et al 2004). These nuclear migration defects are consistent with the model that lamin serves an evolutionarily conserved role as a molecular nut and washer during many nuclear migration events in developing tissues. Defects in human lamin B have been associated with disease, although nowhere near to the extent of lamin A mutations (Coffinier et al., 2010b; Worman, 2012). A duplication of *LMNB1* is associated with a leukodystrophy where myelin is progressively lost (Padiath et al., 2006). Mutations in the *LMNB2* gene are linked to a lipodystrophy (Hegele et al., 2006). Given the mouse knockout phenotypes, it is likely that additional mutations in *LMNB1* and *LMNB2* will be found to be associated with neuronal diseases (Coffinier et al., 2010b).

The nucleoskeleton is a complex network consisting of lamins, inner nuclear membrane proteins and small proteins that link the nuclear envelope to chromatin (Simon and Wilson, 2011). It is therefore unlikely that lamin B is the only component of the molecular nut and washer that dissipates forces throughout the nucleoskeleton during nuclear migration. Obvious candidates to participate with lamins during nuclear migration include the LEM proteins, Baf, and Ima1/NET5/Samp1. In *C. elegans,* mutations in *baf-1* or double mutations in *emr-1* and *lem-2* phenocopy all previously described *lmn-1* phenotypes (Liu et al., 2003; Margalit et al., 2005; Meyerzon et al., 2009b). We were therefore surprised that disrupting in *baf-1* or *emr-1* and *lem-2* did not lead to a nuclear migration phenotype. The inner nuclear membrane protein Ima1/NET5/Samp1 was previously shown to play a role in nuclear migration in mammalian tissue culture cells (Borrego-Pinto et al., 2012). It was also shown to interact with a SUN protein in both yeast and mammalian tissue culture (Borrego-Pinto et al., 2012; Hiraoka et al., 2011). Here we showed that the *C. elegans* homolog SAMP-1 plays a minor role in nuclear migration. Interestingly, we found despite the requirement of Lamin A/C in tissue culture (Borrego-Pinto et al., 2012), *C. elegans* SAMP-1 localized independently of LMN-1. The SAMP-1 binding partners in the *C. elegans* nuclear envelope remain to be determined (question marks in Figure 8A). We suspect that *baf-1*, *emr-1*, *lem-2*, *samp-1*, and other components of the nucleoskeleton play partially redundant roles with lamin during nuclear migration. Therefore, characterization of how the network of proteins forming the nucleoskeleton functions as a unit during nuclear migration requires further investigation.

Materials and Methods

C. elegans strains and RNAi

C. elegans were cultured using standard conditions, and N2 was used as wild type (Brenner, 1974). Some nematode strains used in this work were provided by the Caenorhabditis

Genetics Center, which is funded by the National Institutes of Health National Center for Research Resources. The *unc-84(n322), unc-84(e1174), unc-84(e1411),* and *unc-84(n369)* alleles, from strains MT322, CB1174, CB1411 and MT369, respectively, were previously described (Malone et al., 1999). The construct pSL589 was created by cloning the *Xma*I/*Sph*I fragment of the *col-10* promoter from pOS12 (Spencer et al., 2001) into pPD96.04 to specifically drive expression of NLS::GFP::LacZ in embryonic hypodermal cells. This construct, pSL589, was injected into N2 worms and then integrated (Kage-Nakadai et al., 2012) to create strain UD469 (*ycIs10[$p_{col\text{-}10}$nls::gfp::lacZ]*). This outcrossed line was then crossed to *unc-84(n322), unc-84(e1174), unc-84(e1411),* and *unc-84(n369)* strains to create UD414, UD412, UD396, and UD399 respectively. UD87, expressing the full-length UNC-84 rescue construct, was used as the starting strain for SAMP-1 localization studies in *lmn-1(RNAi)* (Chang et al., 2013; McGee et al., 2006). The *lem-2(tm1582)* deletion strain FX1582 and the *samp-1(tm2710)* deletion strain FX2710 were kindly supplied by Shohei Mitani (National Bioresource Project at the Tokyo Women's Medical University). *samp-1(tm2710)* was balanced with *mIn1 [dpy-10(e128) mIs14] II* from strain BS3493 to make strain UD470. The $p_{lbp\text{-}1}$ *lmn-1::gfp* strain UD324 was previously described (Fridolfsson and Starr, 2010). UD324 was crossed to the *unc-84(n369)* and *unc-84(e1411)* strains above to create UD437 and UD436 respectively.

For the *lmn-1(RNAi)* experiments, *ycIs10* animals in an otherwise wild-type background were staged for 24 hours post L4 at 20°C and fed bacteria expressing dsRNA against *lmn-1* from the Ahringer library (Fraser et al., 2000).Worms were transferred after 24 hours and the plate from the first 24 hours was counted at 48 hours. For *emr-1(RNAi); lem-2(1582)* treatment the first 24 hours were discarded and the second day was counted at 72 hours (Meyerzon et al., 2009b). Empty vector L4440 was used as control RNAi for all feeding experiments. For *baf-1(RNAi),* dsRNA was transcribed *in vitro* from the EST yk333d11 and subsequently injected into young adults (Meyerzon et al., 2009b). Progeny laid from 12-24 hours post injection were screened. RNAi efficiency was assessed by progeny inviability.

Yeast two-hybrid

Constructs expressing GAL-4 DNA Binding Domain::UNC-84 fusion proteins for yeast two-hybrid baits were created by amplifying inserts with PCR from the *unc-84* cDNA, yk402g1 (Kohara, 1996; McGee et al., 2006) and cloning the inserts into pDEST32 using Gateway Technology (Invitrogen). pSL242 expresses residues 1-385 of UNC-84, pSL244 has 59-385, pSL593 has 1-100, pSL592 has 1-59, and pSL595 has residues 385-510 of UNC-84. The P91S mutation was introduced into pSL242 using PCR SOEing to create the mutant bait construct pSL596. The ProQuest *C. elegans* mixed stage cDNA library (Invitrogen) was screened using the UNC-84(1-385) as a bait as previously described (Fridolfsson et al., 2010). Positives with candidate interacting partners were selected on SD-W-L-H. To map the LMN-1 interaction domain of UNC-84, full length LMN-1 prey, pSL719 obtained from the screen, was transformed into yeast strain Y187 (Clontech Laboratories, Inc.). The various UNC-84 baits were transformed into yeast strain Y2HGold (Clontech Laboratories, Inc.). The bait strains were then mated to the prey-containing Y187 strains. Spot assays were conducted by spotting 2μL of yeast serial dilutions; growth was then imaged with an AlphaImager^{TM}3400 (Alpha Innotech Corporation). Liquid β-galactosidase assays were conducted following Clontech protocol PT1020-1 (Schneider et al., 1996).

uclear migration assays

To count abnormally positioned hyp7 nuclei in the dorsal cord, L1 animals carrying *ycIs10[nls::gfp::lacZ]* were examined on a 2% agar pad in M9 solution with 1mM tetramisole (Starr et al., 2001). DIC time-lapse imaging of migrating embryonic hypodermal nuclei was performed as previously reported (Fridolfsson and Starr, 2010). Images were taken every 15 seconds; time zero was defined as the time cell 12 hit the opposite seam cell boundary (Fridolfsson and Starr, 2010). Nuclear position was determined by measuring the leading edge, lagging edge, and midpoint of migrating nuclei using the manual tracking plugin for ImageJ (National Institutes of Health). The distance a nucleus migrated in the first 10 minutes determined in a cell-specific manner such that time zero was when the respective cell's leading edge reached the opposite seam cell boundary. Images were obtained using DIC optics and a 63x Plan Apo 1.40 NA objective on a Leica DM6000 compound microscope equipped with a Leica DC350 camera operated by Leica LAS AF software. Images were processed using ImageJ software available from National Institutes of Health.

LMN-1::GFP time-lapse images were captured at a frame rate of 1/sec using the 488-nm laser on a spinning disc confocal microscope (Marianas Real Time Confocal SDC Workstation; Intelligent Imaging Innovations), using a scan head (CSU-X1: Yokogawa), an auto-focusing laser, Definite Focus (Zeiss), and a modified electron multiplying charge-coupled device camera (Cascade QuantEM 512SC; Photometrics). A 63X NA 1.4 oil immersion objective was used (Carl Zeiss, Inc.). Images were acquired using SlideBook software (version 5.5; Intelligent Imaging Innovations).

Antibodies and immunofluorescence

Polyclonal antibodies (HJA2) against the *C. elegans* SAMP-1 were raised in rabbits injected with his-NusA-tagged C-terminal fragment of SAMP-1 comprising residues 338-555. SAMP-1 antibodies were affinity purified using the same C-terminal SAMP-1 fragment tagged with GST. For immunofluorescence, embryos were extruded from hermaphrodites, permeabilized by the freeze-crack method, fixed for 10 min in -20˚C methanol, blocked in PBST (PBS and 0.1% triton X-100) with 5% milk, and stained as previously described (Miller and Shakes, 1995). The rabbit antibody against SAMP-1 was diluted 1:200 in PBS. UNC-83 monoclonal 1209D7D5 was used undiluted (Starr et al. 2001). UNC-84 IgM monoclonal L 72 6 was diluted 1:100 in PBS (Cain et al., 2014). Alexa Fluor antibodies 594 donkey anti-rabbit IgG, goat 488 anti-mouse IgM and 488 goat anti-mouse IgG diluted 1:500 (Life Technologies, Carlsbad, CA) were used as secondary antibodies. DNA was visualized by a 5 min stain in 1 μg/ml DAPI in PBS.

Acknowledgments

We thank Kevin Hart for generating the integrated hypodermal GFP::NLS transgenic strain, and Ben Lorton, Allen Wang and Joe Nguyen for assistance in the two-hybrid screen. We thank Heidi Fridolfsson, Michael Paddy, and the MCB imaging Facility at UC Davis for advice and assistance in microscopy. We thank David Fay and Dan Levy (University of Wyoming) for helpful discussions and hosting D.A.S. on sabbatical. We thank members of the Starr lab and our colleagues in MCB at UC Davis for helpful discussions. C.R.B. was supported by NIH training

grant T32 GM007377. This study was supported by grant R01 GM073874 from the NIH/NIGMS.

References

Altun, Z.F.a.H., D.H. 2009. Epithelial system, hypodermis. *In* WormAtlas, ed.

Borrego-Pinto, J., T. Jegou, D.S. Osorio, F. Aurade, M. Gorjanacz, B. Koch, I.W. Mattaj, and E.R. Gomes. 2012. Samp1 is a component of TAN lines and is required for nuclear movement. *Journal of cell science*. 125:1099-1105.

Bruusgaard, J.C., K. Liestol, and K. Gundersen. 2006. Distribution of myonuclei and microtubules in live muscle fibers of young, middle-aged, and old mice. *Journal of applied physiology*. 100:2024-2030.

Buch, C., R. Lindberg, R. Figueroa, S. Gudise, E. Onischenko, and E. Hallberg. 2009. An integral protein of the inner nuclear membrane localizes to the mitotic spindle in mammalian cells. *Journal of cell science*. 122:2100-2107.

Burke, B., and K.J. Roux. 2009. Nuclei take a position: managing nuclear location. *Developmental cell*. 17:587-597.

Cain, N.E., E.C. Tapley, K.L. McDonald, C. B.M., and D.A. Starr. 2014. The SUN protein UNC-84 is required only in force-bearing cells to maintain nuclear envelope architecture. *The Journal of cell biology*. 206.

Chang, Y.T., D. Dranow, J. Kuhn, M. Meyerzon, M. Ngo, D. Ratner, K. Warltier, and D.A. Starr. 2013. toca-1 is in a novel pathway that functions in parallel with a SUN-KASH nuclear envelope bridge to move nuclei in Caenorhabditis elegans. *Genetics*. 193:187-200.

Chen, C.Y., Y.H. Chi, R.A. Mutalif, M.F. Starost, T.G. Myers, S.A. Anderson, C.L. Stewart, and K.T. Jeang. 2012. Accumulation of the inner nuclear envelope protein sun1 is pathogenic in progeric and dystrophic laminopathies. *Cell*. 149:565-577.

Chen, Z.J., W.P. Wang, Y.C. Chen, J.Y. Wang, W.H. Lin, L.A. Tai, G.G. Liou, C.S. Yang, and Y.H. Chi. 2014. Dysregulated interactions between lamin A and SUN1 induce abnormalities in the nuclear envelope and endoplasmic reticulum in progeric laminopathies. *Journal of cell science*. 127:1792-1804.

Chow, K.H., R.E. Factor, and K.S. Ullman. 2012. The nuclear envelope environment and its cancer connections. *Nature reviews. Cancer*. 12:196-209.

Coffinier, C., S.Y. Chang, C. Nobumori, Y. Tu, E.A. Farber, J.I. Toth, L.G. Fong, and S.G. Young. 2010a. Abnormal development of the cerebral cortex and cerebellum in the setting of lamin B2 deficiency. *Proceedings of the National Academy of Sciences of the United States of America*. 107:5076-5081.

Coffinier, C., L.G. Fong, and S.G. Young. 2010b. LINCing lamin B2 to neuronal migration: growing evidence for cell-specific roles of B-type lamins. *Nucleus*. 1:407-411.

Coffinier, C., H.J. Jung, C. Nobumori, S. Chang, Y. Tu, R.H. Barnes, 2nd, Y. Yoshinaga, P.J. de Jong, L. Vergnes, K. Reue, L.G. Fong, and S.G. Young. 2011. Deficiencies in lamin B1 and lamin B2 cause neurodevelopmental defects and distinct nuclear shape abnormalities in neurons. *Molecular biology of the cell*. 22:4683-4693.

Crisp, M., Q. Liu, K. Roux, J.B. Rattner, C. Shanahan, B. Burke, P.D. Stahl, and D. Hodzic. 2006. Coupling of the nucleus and cytoplasm: role of the LINC complex. *The Journal of cell biology*. 172:41-53.

Dittmer, T.A., and T. Misteli. 2011. The lamin protein family. *Genome biology*. 12:222.
Folker, E.S., C. Ostlund, G.W. Luxton, H.J. Worman, and G.G. Gundersen. 2011. Lamin A variants that cause striated muscle disease are defective in anchoring transmembrane actin-associated nuclear lines for nuclear movement. *Proceedings of the National Academy of Sciences of the United States of America*. 108:131-136.
Franke, W.W., U. Scheer, G. Krohne, and E.D. Jarasch. 1981. The nuclear envelope and the architecture of the nuclear periphery. *The Journal of cell biology*. 91:39s-50s.
Fraser, A.G., R.S. Kamath, P. Zipperlen, M. Martinez-Campos, M. Sohrmann, and J. Ahringer. 2000. Functional genomic analysis of C. elegans chromosome I by systematic RNA interference. *Nature*. 408:325-330.
Fridkin, A., E. Mills, A. Margalit, E. Neufeld, K.K. Lee, N. Feinstein, M. Cohen, K.L. Wilson, and Y. Gruenbaum. 2004. Matefin, a Caenorhabditis elegans germ line-specific SUN-domain nuclear membrane protein, is essential for early embryonic and germ cell development. *Proc Natl Acad Sci USA*. 101:6987-6992.
Fridolfsson, H.N., N. Ly, M. Meyerzon, and D.A. Starr. 2010. UNC-83 coordinates kinesin-1 and dynein activities at the nuclear envelope during nuclear migration. *Developmental biology*. 338:237-250.
Fridolfsson, H.N., and D.A. Starr. 2010. Kinesin-1 and dynein at the nuclear envelope mediate the bidirectional migrations of nuclei. *The Journal of cell biology*. 191:115-128.
Fu, Y., L.K. Chin, T. Bourouina, A.Q. Liu, and A.M. VanDongen. 2012. Nuclear deformation during breast cancer cell transmigration. *Lab on a chip*. 12:3774-3778.
Gruenbaum, Y., A. Margalit, R.D. Goldman, D.K. Shumaker, and K.L. Wilson. 2005. The nuclear lamina comes of age. *Nature reviews. Molecular cell biology*. 6:21-31.
Gundersen, G.G., and H.J. Worman. 2013. Nuclear positioning. *Cell*. 152:1376-1389.
Gunsalus, K.C., H. Ge, A.J. Schetter, D.S. Goldberg, J.D. Han, T. Hao, G.F. Berriz, N. Bertin, J. Huang, L.S. Chuang, N. Li, R. Mani, A.A. Hyman, B. Sonnichsen, C.J. Echeverri, F.P. Roth, M. Vidal, and F. Piano. 2005. Predictive models of molecular machines involved in Caenorhabditis elegans early embryogenesis. *Nature*. 436:861-865.
Haque, F., D.J. Lloyd, D.T. Smallwood, C.L. Dent, C.M. Shanahan, A.M. Fry, R.C. Trembath, and S. Shackleton. 2006. SUN1 interacts with nuclear lamin A and cytoplasmic nesprins to provide a physical connection between the nuclear lamina and the cytoskeleton. *Molecular and cellular biology*. 26:3738-3751.
Haque, F., D. Mazzeo, J.T. Patel, D.T. Smallwood, J.A. Ellis, C.M. Shanahan, and S. Shackleton. 2010. Mammalian SUN protein interaction networks at the inner nuclear membrane and their role in laminopathy disease processes. *The Journal of biological chemistry*. 285:3487-3498.
Hegele, R.A., H. Cao, D.M. Liu, G.A. Costain, V. Charlton-Menys, N.W. Rodger, and P.N. Durrington. 2006. Sequencing of the reannotated LMNB2 gene reveals novel mutations in patients with acquired partial lipodystrophy. *American journal of human genetics*. 79:383-389.
Hiraoka, Y., H. Maekawa, H. Asakawa, Y. Chikashige, T. Kojidani, H. Osakada, A. Matsuda, and T. Haraguchi. 2011. Inner nuclear membrane protein Ima1 is dispensable for intranuclear positioning of centromeres. *Genes to cells : devoted to molecular & cellular mechanisms*. 16:1000-1011.

Kage-Nakadai, E., H. Kobuna, O. Funatsu, M. Otori, K. Gengyo-Ando, S. Yoshina, S. Hori, and S. Mitani. 2012. Single/low-copy integration of transgenes in Caenorhabditis elegans using an ultraviolet trimethylpsoralen method. *BMC biotechnology*. 12:1.

Kohara, Y. 1996. [Large scale analysis of C. elegans cDNA]. *Tanpakushitsu kakusan koso. Protein, nucleic acid, enzyme*. 41:715-720.

Kracklauer, M.P., S.M. Banks, X. Xie, Y. Wu, and J.A. Fischer. 2007. Drosophila klaroid encodes a SUN domain protein required for Klarsicht localization to the nuclear envelope and nuclear migration in the eye. *Fly*. 1:75-85.

Lee, K.K., D. Starr, M. Cohen, J. Liu, M. Han, K.L. Wilson, and Y. Gruenbaum. 2002. Lamin-dependent localization of UNC-84, a protein required for nuclear migration in Caenorhabditis elegans. *Molecular biology of the cell*. 13:892-901.

Liu, J., K.K. Lee, M. Segura-Totten, E. Neufeld, K.L. Wilson, and Y. Gruenbaum. 2003. MAN1 and emerin have overlapping function(s) essential for chromosome segregation and cell division in Caenorhabditis elegans. *Proceedings of the National Academy of Sciences of the United States of America*. 100:4598-4603.

Liu, J., T. Rolef Ben-Shahar, D. Riemer, M. Treinin, P. Spann, K. Weber, A. Fire, and Y. Gruenbaum. 2000. Essential roles for Caenorhabditis elegans lamin gene in nuclear organization, cell cycle progression, and spatial organization of nuclear pore complexes. *Molecular biology of the cell*. 11:3937-3947.

Luxton, G.G., and D.A. Starr. 2014. KASHing up with the nucleus: novel functional roles of KASH proteins at the cytoplasmic surface of the nucleus. *Current opinion in cell biology*. 28C:69-75.

Luxton, G.W., E.R. Gomes, E.S. Folker, E. Vintinner, and G.G. Gundersen. 2010. Linear arrays of nuclear envelope proteins harness retrograde actin flow for nuclear movement. *Science*. 329:956-959.

Malone, C.J., W.D. Fixsen, H.R. Horvitz, and M. Han. 1999. UNC-84 localizes to the nuclear envelope and is required for nuclear migration and anchoring during C. elegans development. *Development*. 126:3171-3181.

Margalit, A., M. Segura-Totten, Y. Gruenbaum, and K.L. Wilson. 2005. Barrier-to-autointegration factor is required to segregate and enclose chromosomes within the nuclear envelope and assemble the nuclear lamina. *Proceedings of the National Academy of Sciences of the United States of America*. 102:3290-3295.

McGee, M.D., R. Rillo, A.S. Anderson, and D.A. Starr. 2006. UNC-83 IS a KASH protein required for nuclear migration and is recruited to the outer nuclear membrane by a physical interaction with the SUN protein UNC-84. *Molecular biology of the cell*. 17:1790-1801.

Meyerzon, M., H.N. Fridolfsson, N. Ly, F.J. McNally, and D.A. Starr. 2009a. UNC-83 is a nuclear-specific cargo adaptor for kinesin-1-mediated nuclear migration. *Development*. 136:2725-2733.

Meyerzon, M., Z. Gao, J. Liu, J.C. Wu, C.J. Malone, and D.A. Starr. 2009b. Centrosome attachment to the C. elegans male pronucleus is dependent on the surface area of the nuclear envelope. *Developmental biology*. 327:433-446.

Minn, I.L., M.M. Rolls, W. Hanna-Rose, and C.J. Malone. 2009. SUN-1 and ZYG-12, mediators of centrosome-nucleus attachment, are a functional SUN/KASH pair in Caenorhabditis elegans. *Mol Biol Cell*. 20:4586-4595.

Morris, N.R. 2000. Nuclear migration. From fungi to the mammalian brain. *The Journal of cell biology*. 148:1097-1101.

Ostlund, C., E.S. Folker, J.C. Choi, E.R. Gomes, G.G. Gundersen, and H.J. Worman. 2009. Dynamics and molecular interactions of linker of nucleoskeleton and cytoskeleton (LINC) complex proteins. *Journal of cell science*. 122:4099-4108.

Padiath, Q.S., K. Saigoh, R. Schiffmann, H. Asahara, T. Yamada, A. Koeppen, K. Hogan, L.J. Ptacek, and Y.H. Fu. 2006. Lamin B1 duplications cause autosomal dominant leukodystrophy. *Nature genetics*. 38:1114-1123.

Patterson, K., A.B. Molofsky, C. Robinson, S. Acosta, C. Cater, and J.A. Fischer. 2004. The functions of Klarsicht and nuclear lamin in developmentally regulated nuclear migrations of photoreceptor cells in the Drosophila eye. *Molecular biology of the cell*. 15:600-610.

Reinsch, S., and P. Gonczy. 1998. Mechanisms of nuclear positioning. *Journal of cell science*. 111 (Pt 16):2283-2295.

Schirmer, E.C., L. Florens, T. Guan, J.R. Yates, 3rd, and L. Gerace. 2003. Nuclear membrane proteins with potential disease links found by subtractive proteomics. *Science*. 301:1380-1382.

Schneider, S., M. Buchert, and C.M. Hovens. 1996. An in vitro assay of beta-galactosidase from yeast. *BioTechniques*. 20:960-962.

Simon, D.N., and K.L. Wilson. 2011. The nucleoskeleton as a genome-associated dynamic 'network of networks'. *Nature reviews. Molecular cell biology*. 12:695-708.

Sosa, B.A., A. Rothballer, U. Kutay, and T.U. Schwartz. 2012. LINC complexes form by binding of three KASH peptides to domain interfaces of trimeric SUN proteins. *Cell*. 149:1035-1047.

Spencer, A.G., S. Orita, C.J. Malone, and M. Han. 2001. A RHO GTPase-mediated pathway is required during P cell migration in Caenorhabditis elegans. *Proceedings of the National Academy of Sciences of the United States of America*. 98:13132-13137.

Starr, D.A. 2011. Watching nuclei move: Insights into how kinesin-1 and dynein function together. *Bioarchitecture*. 1:9-13.

Starr, D.A. 2012. Laminopathies: too much SUN is a bad thing. *Current biology : CB*. 22:R678-680.

Starr, D.A., and H.N. Fridolfsson. 2010. Interactions between nuclei and the cytoskeleton are mediated by SUN-KASH nuclear-envelope bridges. *Annual review of cell and developmental biology*. 26:421-444.

Starr, D.A., and M. Han. 2002. Role of ANC-1 in tethering nuclei to the actin cytoskeleton. *Science*. 298:406-409.

Starr, D.A., and M. Han. 2005. A genetic approach to study the role of nuclear envelope components in nuclear positioning. *Novartis Foundation symposium*. 264:208-219; discussion 219-230.

Starr, D.A., G.J. Hermann, C.J. Malone, W. Fixsen, J.R. Priess, H.R. Horvitz, and M. Han. 2001. unc-83 encodes a novel component of the nuclear envelope and is essential for proper nuclear migration. *Development*. 128:5039-5050.

Sulston, J.E., and H.R. Horvitz. 1981. Abnormal cell lineages in mutants of the nematode Caenorhabditis elegans. *Developmental biology*. 82:41-55.

Sulston, J.E., E. Schierenberg, J.G. White, and J.N. Thomson. 1983. The embryonic cell lineage of the nematode Caenorhabditis elegans. *Developmental biology*. 100:64-119.

Tapley, E.C., N. Ly, and D.A. Starr. 2011. Multiple mechanisms actively target the SUN protein UNC-84 to the inner nuclear membrane. *Molecular biology of the cell*. 22:1739-1752.

Tapley, E.C., and D.A. Starr. 2013. Connecting the nucleus to the cytoskeleton by SUN-KASH bridges across the nuclear envelope. *Current opinion in cell biology*. 25:57-62.

Tsai, J.W., K.H. Bremner, and R.B. Vallee. 2007. Dual subcellular roles for LIS1 and dynein in radial neuronal migration in live brain tissue. *Nature neuroscience*. 10:970-979.

Turgay, Y., R. Ungricht, A. Rothballer, A. Kiss, G. Csucs, P. Horvath, and U. Kutay. 2010. A classical NLS and the SUN domain contribute to the targeting of SUN2 to the inner nuclear membrane. *The EMBO journal*. 29:2262-2275.

Wang, X., Y. Zhao, K. Wong, P. Ehlers, Y. Kohara, S.J. Jones, M.A. Marra, R.A. Holt, D.G. Moerman, and D. Hansen. 2009. Identification of genes expressed in the hermaphrodite germ line of C. elegans using SAGE. *BMC genomics*. 10:213.

Worman, H.J. 2012. Nuclear lamins and laminopathies. *The Journal of pathology*. 226:316-325.

Zhang, X., and M. Han. 2010. Nuclear migration: rock and roll facilitated by dynein and kinesin. *Current biology : CB*. 20:R1027-1029.

Zhang, X., K. Lei, X. Yuan, X. Wu, Y. Zhuang, T. Xu, R. Xu, and M. Han. 2009. SUN1/2 and Syne/Nesprin-1/2 complexes connect centrosome to the nucleus during neurogenesis and neuronal migration in mice. *Neuron*. 64:173-187.

Zhou, K., and W. Hanna-Rose. 2010. Movers and shakers or anchored: Caenorhabditis elegans nuclei achieve it with KASH/SUN. *Developmental dynamics : an official publication of the American Association of Anatomists*. 239:1352-1364.

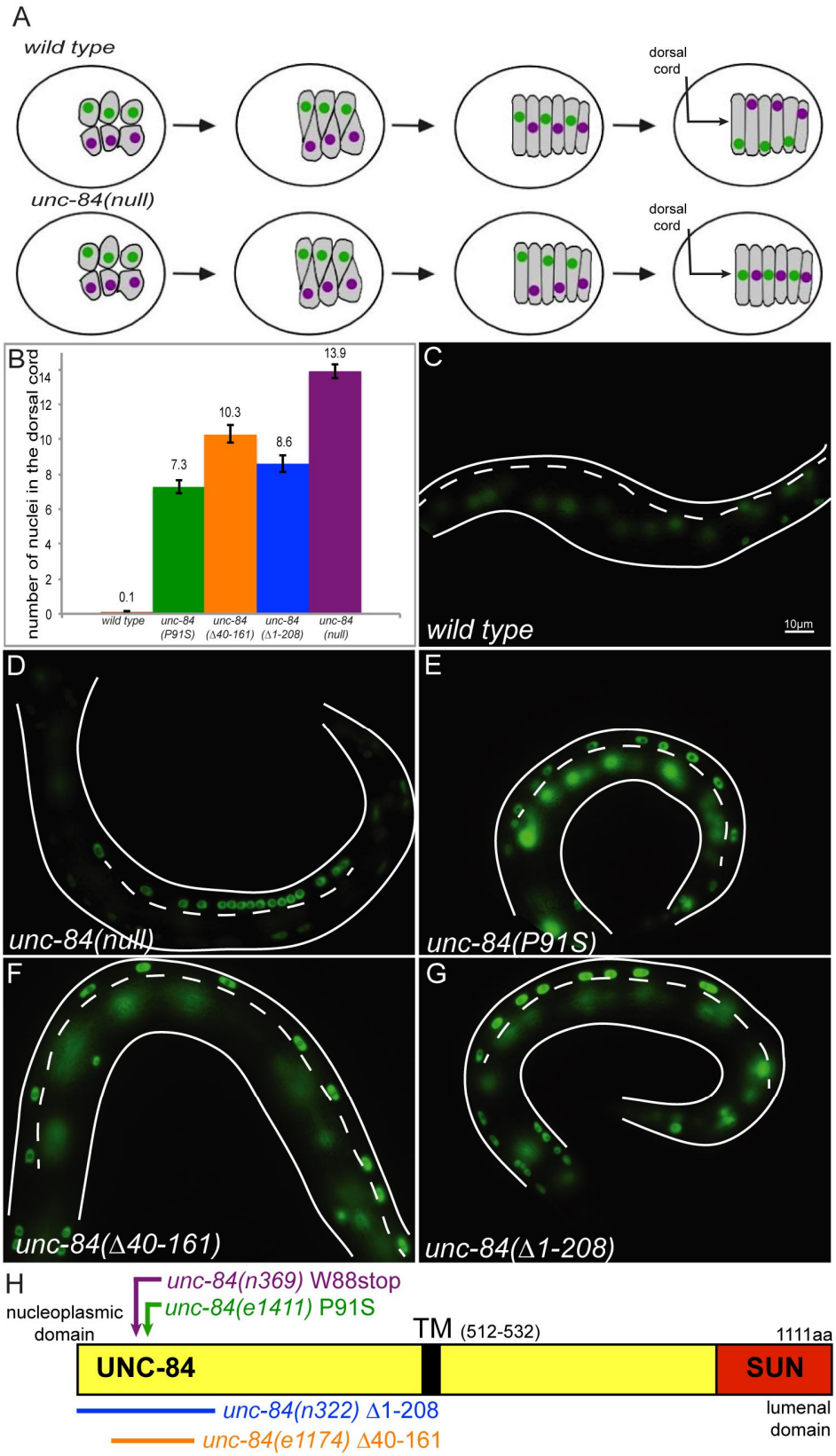
A
wild type
dorsal cord
unc-84(null)
dorsal cord
B
number of nuclei in the dorsal cord
0
2
4
6
8
10
12
14
0.1
7.3
10.3
8.6
13.9
wild type
unc-84 (P91S)
unc-84 (Δ40-161)
unc-84 (Δ1-208)
unc-84 (null)
C
wild type
10μm
D
unc-84(null)
E
unc-84(P91S)
F
unc-84(Δ40-161)
G
unc-84(Δ1-208)
H
nucleoplasmic domain
unc-84(n369) W88stop
unc-84(e1411) P91S
TM (512-532)
1111aa
UNC-84
SUN
unc-84(n322) Δ1-208
unc-84(e1174) Δ40-161
lumenal domain

Figure 1. Mutations in the nucleoplasmic domain of UNC-84 lead to an intermediate nuclear migration defect. (A) A cartoon describes hyp7 precursor nuclear migration on the dorsal surface of the precomma-stage embryo. In wild-type embryos (top), two rows of hyp7 precursors (gray) intercalate to form a row of column shaped cells. Nuclei then migrate from right to left (green) or left to right (purple). In *unc-84(null)* mutant embryos, intercalation occurs normally, but the nuclei fail to migrate. Instead, underlying body wall muscle migrations push *unc-84* nuclei to the dorsal cord (arrow). The dorsal surface is shown; anterior is left. (B) The average number of nuclei present in the dorsal cord of L1 larvae, which approximates the number of failed nuclear migrations, is shown. Error bars show the 95% confidence interval. (C-G) The number of nuclei in the larval dorsal cord were counted following hypodermal nuclei that express a nucleoplasmic GFP from *ycIs10[*$p_{col\text{-}10}$*nls::gfp::lacZ]*. Lateral views of L1 larvae are shown. Dorsal is up and anterior is left; the dorsal cord (arrow in A) is demarcated by the white dotted line. The scale bar is 10 μm. Representative images are shown of (C) wild type, (D) *unc-84(null)*, (E) *unc-84(P91S)*, (F) *unc-84(Δ40-161)*, and (G) *unc-84(Δ1-208)*. (H) A schematic of the domain structure of UNC-84. The conserved SUN domain is red and the trans-membrane span is black. The mutants discussed in the text are indicated.

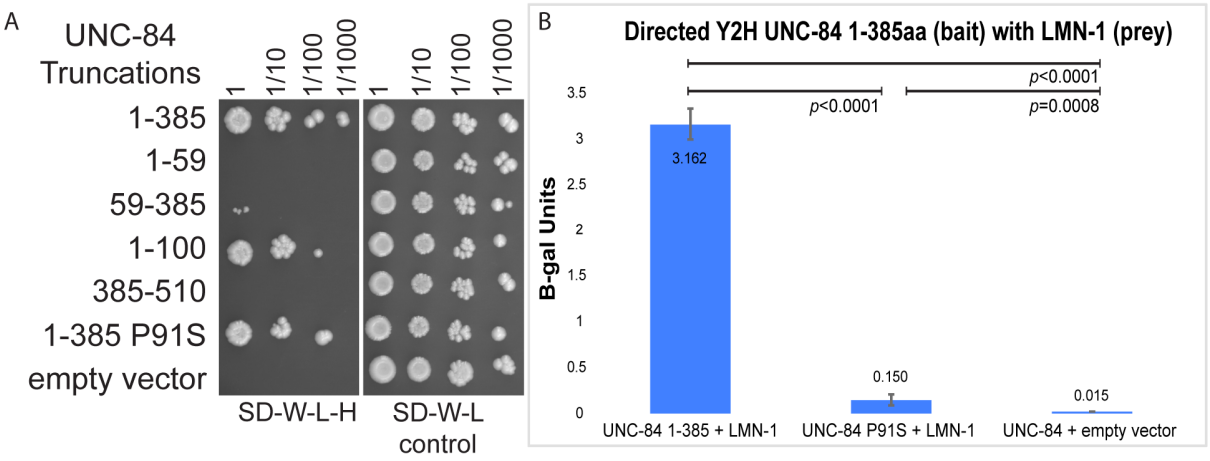

Figure 2. UNC-84 and LMN-1 interact in a yeast two-hybrid assay. (A) Yeast growing in a directed yeast two-hybrid assay are shown. All yeast express the LMN-1::Gal4AD prey construct and the UNC-84::Gal4BD bait construct indicated on the left. Yeast were grown to the same concentration, serially diluted (as indicated at the top) and plated on SD-W, L, and H media that requires an interaction to grow (left panel), or SD-W, and L media as control (right panel). (B) Activity of the *lacZ* gene as activated by a liquid ONPG assay that represents a two-hybrid interaction is shown. Average β-galactosidase units (ΔOD_{420}/min*ml of cells) from three different experiments, each done in triplicate, and the associated 95% confidence interval error bars are shown. Significant statistical differences are noted on the top as determined by student t-tests.

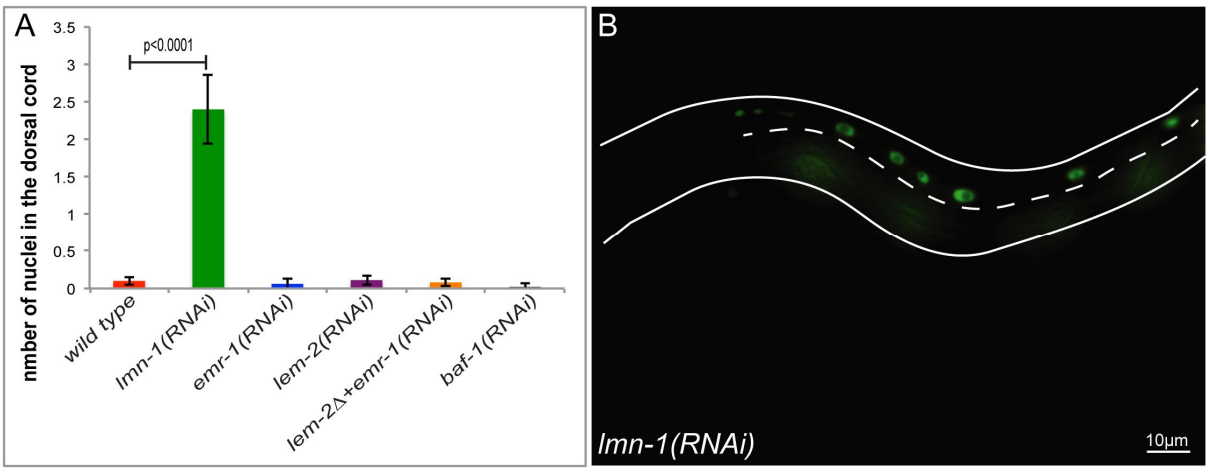

Figure 3. *lmn-1(RNAi)* animals have a nuclear migration defect. (A) The mean number of nuclei present in the dorsal cord of wild type, *lmn-1(RNAi)*, *emr-1(RNAi)*, *lem-2(RNAi)*, *lem-2(tm1582); emr-1(RNAi)*, and *baf-1(RNAi)* are depicted. Error bars represent the 95% confidence interval. (B) A representative *lmn-1(RNAi)* L1 larva depicting nuclei in the dorsal cord which have failed to migrate. The dashed line marks the dorsal cord, anterior is to the left, and dorsal is up. The scale bar is 10 µm.

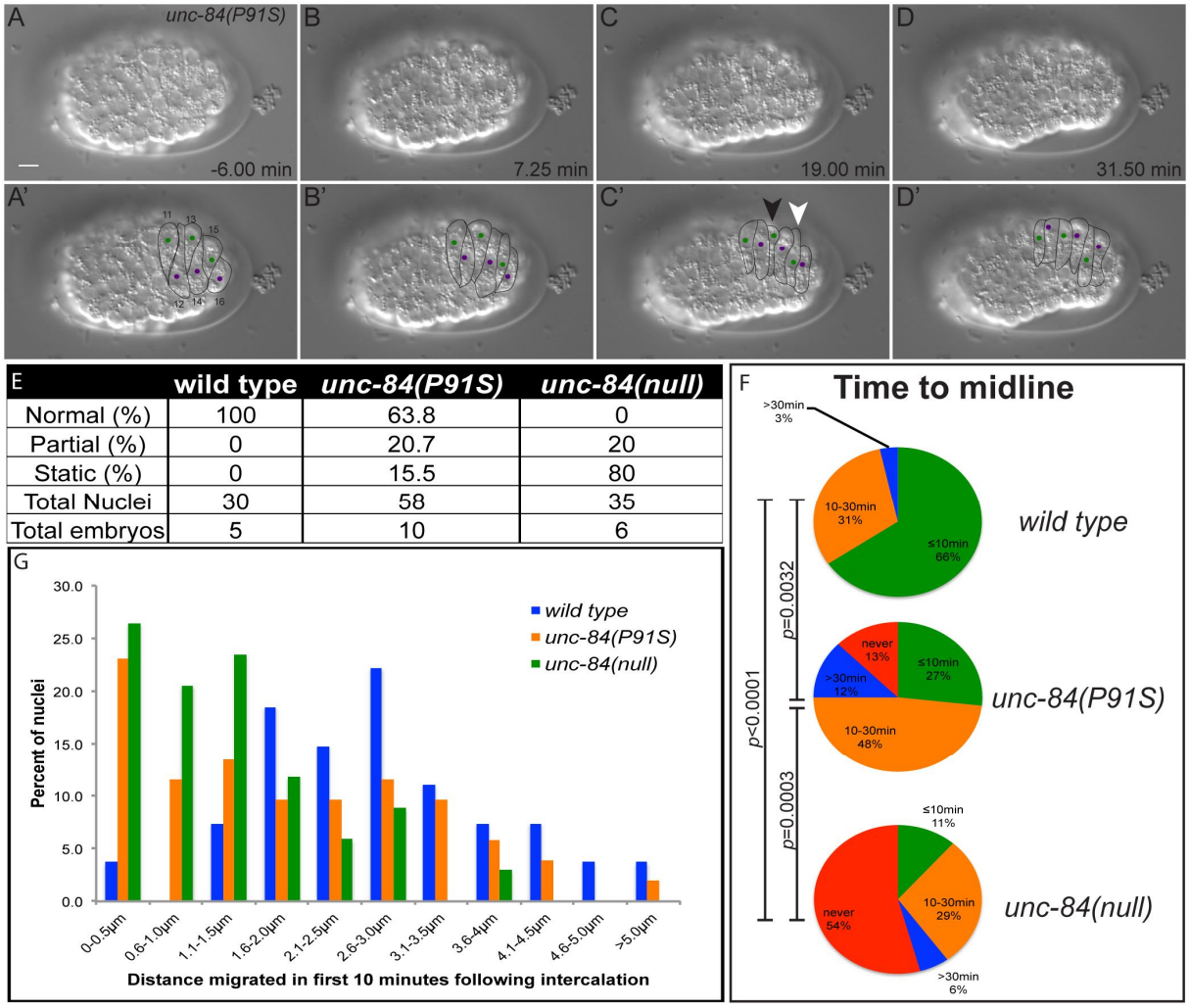

Figure 4. Time-lapse imaging of *unc-84* mutant nuclear migration events. (A-D) A time-lapse series showing nuclear migration in an *unc-84(P91S)* mutant embryo. Dorsal views with anterior on the left are shown. The top row shows raw DIC images, while cell-cell boundaries and nuclei are marked in the bottom row. The green nuclei in cells 11, 13, and 15 migrate from right to left and the purple nuclei in cells 12, 14, and 16 migrate left to right. The nucleus of cell 13 (white arrowhead) fails to migrate, while the nucleus in cell 15 (black arrowhead) migrated half way across and then stopped. Scale bar is 50µm. This is the same embryo as in supplemental movie 3. (E) Quantification of the percent of nuclei that migrated normally, initiated nuclear migration but failed to complete it (partial), or failed to move at all (static). (F) Quantification of the time it took nuclei to reach the dorsal midline of the embryo. Nuclei were categorized into those that reached the midline within 10 min of the completion of intercalation (green), 10-30 min (orange), greater than 30 min (blue), or never (red). Significant statistical differences are noted on the left as determined by χ^2 contingency tests. (G) The distance a nucleus traveled in the first 10 minutes after the completion of intercalation is plotted in a histogram. Each individual nucleus was binned into 0.5 µm increments.

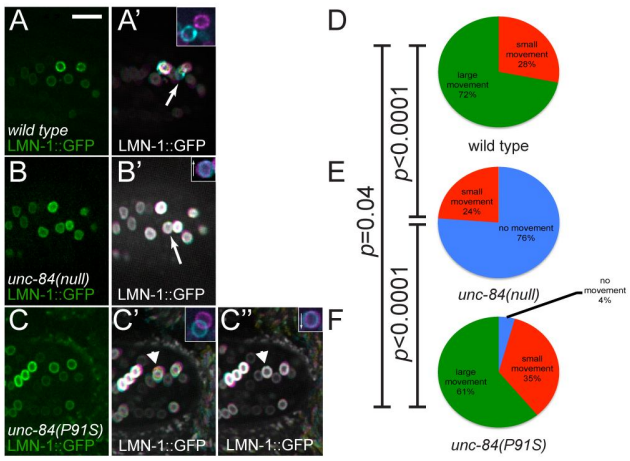

Figure 5. LMN-1::GFP shows dynamic nuclear morphology during nuclear migration. (A-C) Images of embryos expressing LMN-1::GFP specifically in hypodermal cells at the start of time-lapse imaging are depicted. Dorsal views, anterior is left. Insets show the identified nucleus at the beginning (magenta) and end (cyan) of the 8 min 20 sec film. Arrows in insets show the direction the nucleus is supposed to me moving. (A) wild type, (B) *unc-84(null),* and (C) *unc-84(P91S)* embryos. (A'-C') Time projections of 500 frames taken at one second intervals are depicted. In these projections frames 1-166 are colored magenta, 167-333 are yellow, and frames 334-500 are cyan to show the direction of movement (Figure 5 A'-C'). A second time-lapse projection of the same embryo is shown for *unc-84(P91S)* (C''). The arrowheads in C' and C'' mark a *unc-84(P91S)* nucleus that was migrating normally in time-lapse 1 (C'), but then failed to continue migration in time-lapse 2 (C''). Scale bar is 10µm. (D-F) Nuclei were classified into three categories, no movement, small movement, and large movement. The percentage in each category is depicted. Significant statistical differences are noted on the left as determined by χ^2 contingency tests. The arrow in A' is an example of a large movement and the arrow in B' demonstrates no movement.

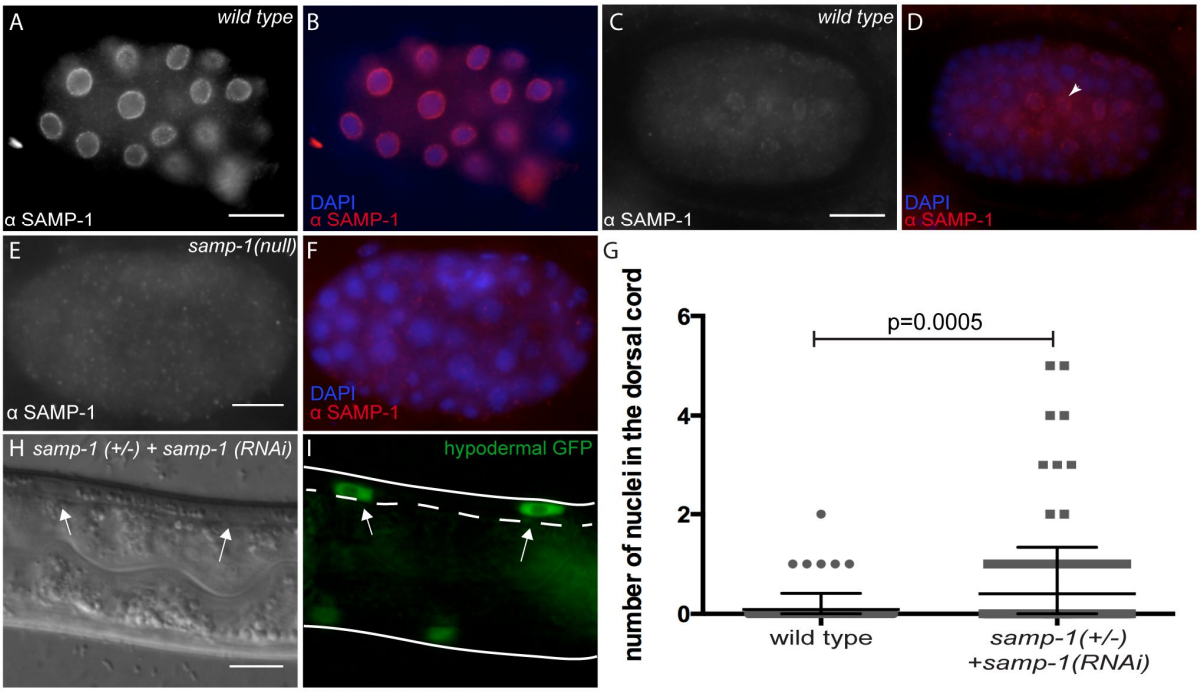

Figure 6. *samp-1(RNAi)* animals have a weak nuclear migration defect. (A-F) Embryos were stained for SAMP-1 localization. Lateral views are shown with anterior left and dorsal up. The scale bars are 10 μm. For each pair of images, SAMP-1 immunostaining is shown in white on the left and in red on the right when it is merged with DAPI staining of nuclei in blue. (A-B) an early wild-type embryo. (C-D) A later, pre-comma stage embryo is shown. Arrowhead points to a hyp7 precursor nucleus. (E-F) A *samp-1(tm2710)* null embryo is shown to demonstrate specificity of the antibody. (G) The numbers of nuclei in the dorsal cords of wild type or *samp-1(tm2710)/(+); samp-1(RNAi)* L1 larvae are shown. Each gray dot represents an individual animal. The mean and 95% confidence interval error bars are shown. (H-I) DIC and GFP images showing two hyp7 nuclei abnormally in the dorsal cord (arrows) of a *samp-1(tm2710)/(+); samp-1(RNAi)* L1 larvae. The dorsal cord is up and is demarcated by the dotted line. Scale bar is 10 μm

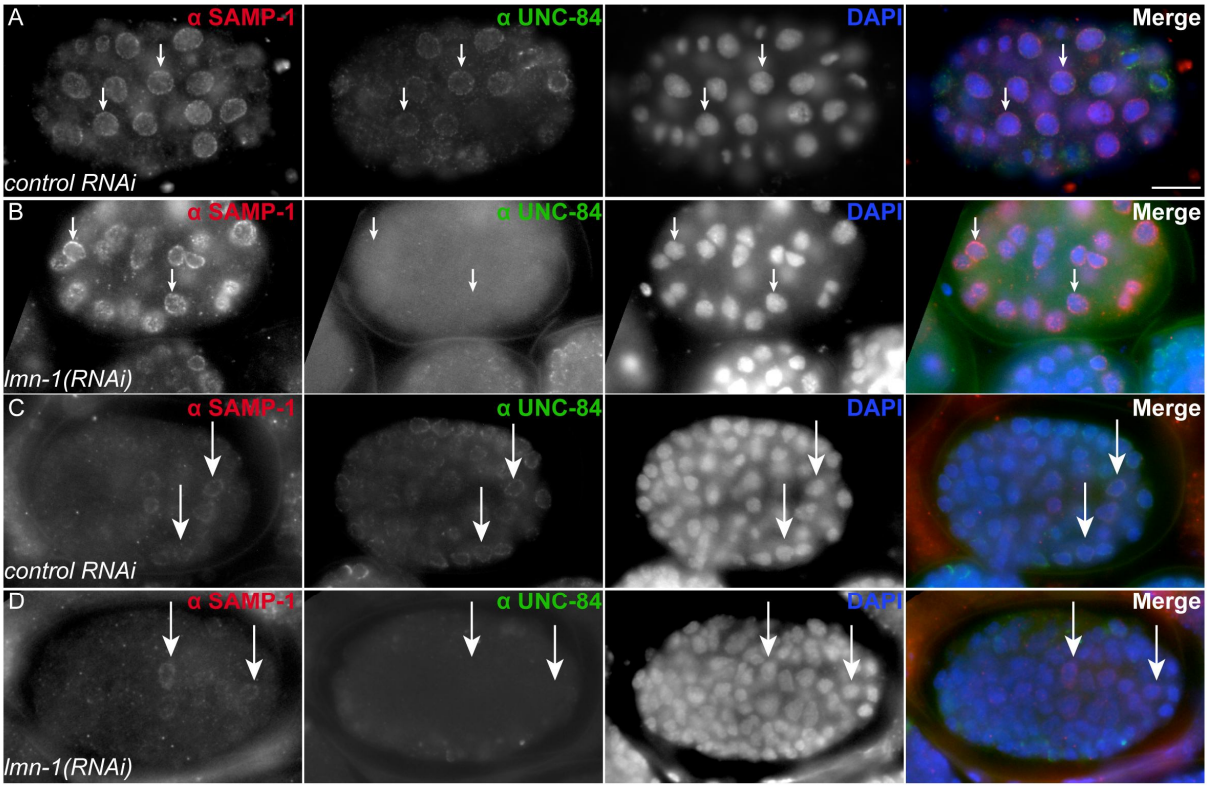

Figure 7. SAMP-1 localizes independently of LMN-1. (A-D) Embryos were stained for SAMP-1 and UNC-84 localization. Lateral views are shown with anterior left and dorsal up. For each row, SAMP-1 immunostaining is shown in white in the left column and in red on the right when all channels are merged. UNC-84 is shown in white in the second column from the left and in green when merged. DAPI staining of nuclei is shown in white in the third column and in blue when merged. (A) An early embryo fed bacteria containing the empty L4440 vector as control. (B) An early embryo fed *lmn-1(RNAi)*. (C) A later, pre-comma stage embryo fed bacteria containing the empty L4440 vector as control. (D) A later, pre-comma stage embryo fed *lmn-1(RNAi)*. Arrows highlight specific nuclei to provide reference points in all four columns. Scale bar is 10 μm.

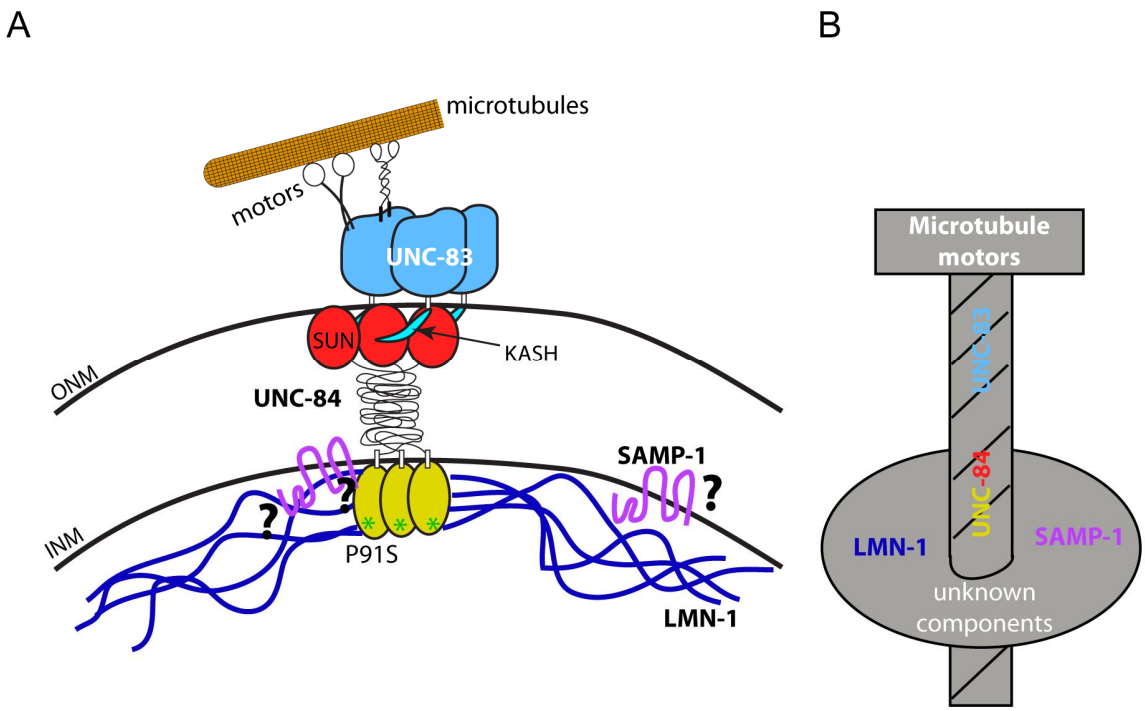

Figure 8. The nut and bolt model for nuclear migration. (A) A cartoon of the KASH/SUN nuclear envelope bridge during nuclear migration. UNC-83 is shown in blue, with the KASH peptide in teal. UNC-84 is shown with the SUN domain in red, the domain spanning the perinuclear space in black, and the nucleoplasmic domain in yellow. The green asterisks symbolize the P91S mutation in UNC-84. LMN-1 is shown in dark blue and SAMP-1 in fuchsia. Microtubule motors are shown in black and white interacting with a single microtubule in orange. Question marks symbolize open questions regarding protein interactions. (B) The bolt and nut/washer analogy is diagramed. The UNC-83/UNC-84 nuclear envelope bridge is represented by a bolt and nucleoskeleton proteins including LMN-1 and SAMP-1 compose the nut/washer.